IEEE Access
Multidisciplinary ⋮ Rapid Review ⋮ Open Access Journal

Received 13 November 2025, accepted 9 December 2025, date of publication 12 December 2025,
date of current version 22 December 2025.

Digital Object Identifier 10.1109/ACCESS.2025.3643644

APPLIED RESEARCH

Evaluation of Stress Response Using Smartphone PPG for Anxiety and Depression Monitoring

DIEGO CAJAL[1,2], CONCEPCIÓN DE LA CÁMARA[3,4], MAR POSADAS-DE MIGUEL[3], NOEL TORRIJOS[5], ÓSCAR NADAL[5], TERESA BLANCO[6], SARA SIDDI[7], PABLO ARMAÑAC[1,2], EDUARDO GIL[1,2], JESÚS LÁZARO[1,2], AND RAQUEL BAILÓN[1,2], (Member, IEEE)

[1]Biomedical Signal Interpretation and Computational Simulation (BSICoS) Group, Aragón Institute of Engineering Research (I3A), IIS Aragón, University of Zaragoza, 50018 Zaragoza, Spain
[2]Centro de Investigación Biomédica en Red en Bioingeniería, Biomateriales y Nanomedicina (CIBER-BBN), 28029 Madrid, Spain
[3]IIS Aragón, 50018 Zaragoza, Spain
[4]Hospital Clínico Universitario, 50009 Zaragoza, Spain
[5]SOS Adolescentes, 22002 Huesca, Spain
[6]Human Open Ware Research Group (Howlab), I3A, University of Zaragoza, 50018 Zaragoza, Spain
[7]Parc Sanitari Sant Joan de Deu, Institut de Recerca Sant Joan de Deu, CIBERSAM, 08830 Barcelona, Spain

Corresponding author: Diego Cajal (dcajal@unizar.es)

This work was supported in part by Ministerio de Ciencia, Innovación y Universidades (MCIN)/Agencia Estatal de Investigación (AEI)/10.13039/501100011033 under Grant PID2024-160041OB-I00 and Grant PID-2022-138585OA-C32, in part by "European Regional Development Fund (ERDF): A way of making Europe," funded by MCIN/AEI/10.13039/501100011033 under Grant PDC2021-120775-I00 and Grant TED2021-131106B-I00, in part by European Union NextGenerationEU/Plan de Recuperación, Transformación y Resiliencia (PRTR), in part by the Gobierno de Aragon (Reference Groups BSICoS T39-23R and Howlab T27-17R; and Better: Project PROY-T38-24), and in part by the University of Zaragoza under Project UZ2022-IAR-06.

ABSTRACT Diminished stress reactivity is frequently reported in individuals with depression and anxiety. Smartphone-camera photoplethysmography (SCPPG) could offer an innovative, objective, and ambulatory metric for monitoring these conditions. This study aims to evaluate the use of SCPPG to monitor anxiety and depression by analyzing stress responses. Specifically, it examines the autonomic nervous system through heart rate variability using pulse rate variability (PRV) metrics derived from SCPPG. The study involved 79 participants, including patients diagnosed with generalized anxiety disorder and major depressive disorder ($n = 22$), as well as a control group ($n = 57$). SCPPG signals were compared with those from a validated device during a stress-inducing protocol, consisting of baseline, stress tests (Trail Making Test and Stroop Test), and recovery phases. Pearson's correlation and Bland-Altman analysis were used to assess the agreement. The results indicate a high correlation ($r \geq 0.96$, $p < 0.001$) between PRV metrics derived from SCPPG and those from reference devices. Additionally, exhibited minimal bias ($\Delta \leq 2\%$) with the exception of RMSSD ($\Delta = 12\%$). Notably, SCPPG reliably detects stress reactivity differences between patient and control groups across all PRV metrics ($p < 0.05$). The study highlights the significance of SCPPG in understanding and personalizing mental health treatments, considering factors such as stress reactivity and recovery. Future research directions include longitudinal studies and improving SCPPG accuracy, particularly for patients with tremors or during dynamic tasks.

INDEX TERMS Anxiety, depression, heart rate variability (HRV), photoplethysmography (PPG), smartphone, stress, wearables.

I. INTRODUCTION

The human body functions as a dynamic system, constantly adjusting to its environment to maintain homeostasis. Interactions with the environment create various situations typically classified as either stressful or relaxing. Beyond the subjective feelings these situations produce, the autonomic nervous system (ANS) regulates energy expenditure during relaxation by decreasing heart rate, expanding blood vessels, and slowing breathing. The opposite processes occur in stressful or threatening situations. Although this physiological response is innate and shared by all mammals, providing

The associate editor coordinating the review of this manuscript and approving it for publication was Angelo Trotta.

an evolutionary advantage [1], [2], it can be affected by factors such as chronic stress, generalized anxiety disorder (GAD), and major depressive disorder (MDD) [2], [3], [4], [5]. Beyond acute autonomic adjustments, psychological stress is associated with endocrine, autonomic, and immune alterations that influence disease risk [6], which motivates objective and scalable stress quantification.

Numerous studies have documented diminished stress reactivity in individuals with depression and anxiety [2], [3], [4], [7], [8], [9], [10], [11], [12], [13]. This hyporeactivity is interpreted as a reduction in parasympathetic withdrawal and parasympathetic overactivation during stress, although the literature on the latter is inconsistent [3]. Some studies, however, indicate increased reactivity [5], [14], [15], [16], while others report both trends depending on the type of stressor [17], [18]. The causality of altered stress reactivity remains unclear: it may be a risk factor for developing GAD and MDD, or these disorders could be the cause. Alternatively, a shared pathway might exist that includes GAD, MDD, and compromised stress reactivity [17], [19].

Understanding the pathophysiology of GAD and MDD is rudimentary compared to other diseases, primarily due to the challenges in studying brain changes [20]. The evaluation of these disorders often relies on subjective assessments, including symptoms that frequently overlap between conditions [20]. Thus, investigating objective metrics to enhance understanding and personalize treatment for depression, anxiety, and related disorders is crucial.

Assessing the ANS through heart rate variability (HRV) provides objective data that complements other techniques, such as neuroimaging. High HRV levels at rest and greater reactivity are associated with attention and emotion processes that facilitate adaptive stress responses, better regulation, and executive function [2]. Moreover, HRV can improve understanding of the interactions among various pathologies with established connections, such as the relationship between depression and sleep apnea or cardiovascular disease, which are also examined through HRV [2], [18], [21].

Initially, the study of HRV focused on electrocardiographic signals. However, pulse photoplethysmography (PPG) has emerged as a popular alternative. Many wearable devices nowadays use PPG to derive a surrogate for HRV, known as Pulse Rate Variability (PRV), that is well known to show high correlation [22]. PPG uses an optical sensor to measure the light passing through tissue over time with a steady light source. Smartphones can capture this signal by using the camera as an optical sensor and the flashlight as an emitter. The ubiquitous presence of smartphones presents significant potential for this technology [23].

This study evaluates the use of smartphone-camera photoplethysmography (SCPPG) to derive PRV metrics for monitoring depression and anxiety. SCPPG signals may exhibit lower quality compared to those obtained from conventional PPG devices. Movements, along with variations in finger pressure on the camera, are the primary factors causing artifacts. Therefore, validation for different applications must be conducted within each specific scenario. SCPPG has previously been validated for obtaining PRV metrics [24], [25] and has been utilized in wellness and healthcare applications [23], [26], [27]. However, to the best of the authors' knowledge, this study represents the first instance of SCPPG being validated in a protocol specifically designed to monitor anxiety and depression.

This study includes a comparison between SCPPG and a validated device within a stress assessment protocol, administered to individuals diagnosed with MDD and/or GAD, as well as a control group. The aim is to determine whether the ANS-related metrics obtained from the SCPPG are consistent with those obtained from the reference device. An initial study demonstrated a strong concordance of PRV metrics in a limited group of healthy individuals [28]. Additionally, this research aims to further evaluate whether SCPPG can accurately identify stress reactivity and if the variations between the patient and control groups align with those observed using the reference device. Successful validation would add a broadly accessible tool to the existing methods for monitoring anxiety and depression.

The novelty of this work is the validation of the PRV metrics using SCPPG in a protocol designed for monitoring anxiety and depression, including tasks involving movement and speech (see Section II-B). These metrics include the sympathovagal balance obtained by orthogonal subspace decomposition of the heart modulation signal from the SCPPG and a respiration signal (see Section II-E), which enhances the accuracy of HRV analysis by separating respiration-related fluctuations [29].

II. METHODS

A. DATASET

A total of 82 individuals participated in a depression assessment protocol. Among them, 24 were diagnosed with GAD and/or MDD (patient group), whereas 58 were healthy individuals (control group). Exclusion criteria ensured that participants in both groups did not have any cardiac, neurological, or endocrine conditions, nor any other psychiatric disorders, to prevent potential confounders. Participants taking tricyclic antidepressants, beta-blockers, and antipsychotics were also excluded due to their effects on the autonomic control of the heart [1], [30], [31], [32]. Out of the 82 participants, 3 individuals (2 patients and 1 control) experienced difficulties with finger stability on the camera due to tremors (this issue is addressed in Section IV). As a result, these participants were excluded from subsequent analyses, leaving a final sample size of 79 subjects, consisting of 22 patients and 57 controls. Patients were recruited by the Hospital ClÍnico Universitario (Zaragoza, Spain) and by SOS Adolescentes (Huesca, Spain), while controls were recruited by social networks.

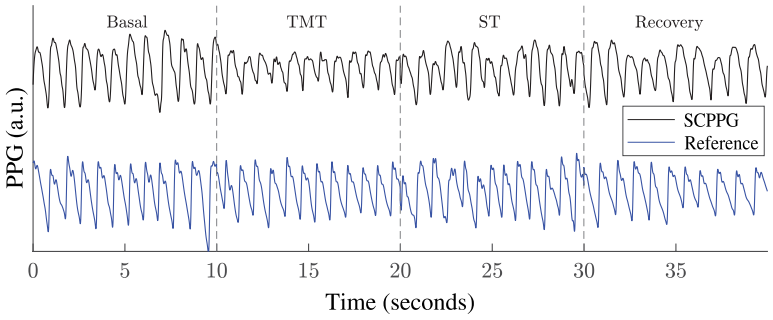

FIGURE 1. SCPPG (black) and reference (blue) signals, expressed in arbitrary units (a.u.). The image consists of 10-second segments extracted from different stages of the protocol, which have been assembled together. The time axis is shown as a reference; it does not indicate continuity.

TABLE 1. Demographic characteristics. Significative differences between paired controls and patients ($p < 0.05$) in bold.

	Group		
	All subjects ($n = 79$)	Paired controls ($n = 22$)	Patient ($n = 22$)
Age, *Mean (SD)*	31 (12)	30 (10)	30 (12)
Age, *Range*	18-66	19-64	18-64
Male, *N (%)*	37 (47%)	5 (23%)	5 (23%)
Weight [kg], *Mean (SD)*	70 (13)	65 (10)	66 (12)
Height [cm], *Mean (SD)*	172 (9)	168 (8)	169 (10)
BMI, *Mean (SD)*	24 (3)	23 (3)	23 (4)
PSS, *Mean (SD)*	15.2 (6.4)	14.3 (5.8)	**20.0 (7.5)**
PSS, *Range*	5-32	5-20	5-32
S-STAI, *Mean (SD)*	17.7 (9.8)	14.9 (6.3)	**24.3 (12.2)**
S-STAI, *Range*	2-50	2-21	6-50
T-STAI, *Mean (SD)*	19.7 (10.7)	16.0 (7.3)	**28.7 (12.7)**
T-STAI, *Range*	3-52	3-24	9-52
ES3, *Mean (SD)*	17.7 (17.0)	8.8 (6.1)	**31.5 (21.0)**
ES3, *Range*	0-69	0-23	2-69
ES3-V, *Mean (SD)*	37.6 (24.7)	37.4 (23.9)	45.6 (28.4)
ES3-V, *Range*	0-95	3-65	0-95

PSS ranges from 0 to 40, S-STAI and T-STAI range from 0 to 60, ES3 ranges from 0 to 80, and ES3-V ranges from 0 to 100.

Participants were instructed to sit down and minimize their movements throughout the procedure. They used their non-dominant hand to hold a Pocophone F1 (Xiaomi Inc.) smartphone and covered the camera with their index finger. The camera's placement on this device, approximately 5 mm to the right of the camera, allows the user to hold the smartphone comfortably without directly touching the flashlight, which can produce uncomfortable heat during prolonged recording sessions. The flashlight remained on during the recordings, and both the autofocus and autoexposure functions of the camera were disabled to prevent nonphysiological oscillations in the SCPPG signal. This step is essential since such oscillations usually occur at a frequency similar to that of the blood pulses and potentially cause confusion.

A Medicom system (Medicom MTD), referred to as the Reference, was simultaneously used to record a conventional PPG signal from the ring finger of the same hand for comparison, with a sampling rate of 250 Hz (see Figure 1). Besides this PPG signal, this device also recorded the respiratory effort from the chest at the same sampling rate. The smartphone app used was created in-house to record SCPPG data using Flutter (Google LLC). The software analyzes the video stream, which has a resolution of 320 × 240 pixels and uses RGB encoding, by summing the green-channel intensity over all pixels in each 320 × 240 frame (full-frame region of interest) to produce a single SCPPG trace. In terms of reproducibility of the results, averaging or summation are equivalent up to a constant scale and do not affect downstream analyses. The frame rate is approximately 24 frames per second, although it can vary based on the operating system's workload. The signal is then upsampled to 250 Hz using cubic splines to match the reference sampling rate, provide a smooth, differentiable representation, and enable consistent sub-frame peak timing within a unified processing pipeline. Interpolation and further processing were conducted offline using MATLAB (MathWorks Inc.). Recordings were exported as CSV files with one row per

frame, including UNIX timestamps (milliseconds) and the RGB intensities; these timestamps defined the time base for subsequent processing.

Before initiating the stress protocol, participants were interviewed to gather their personal information and confirm the inclusion and exclusion criteria. During this interview, participants completed four tests to evaluate their self-perceived stress: the Perceived Stress Scale (PSS), the State-Trait Anxiety Inventory (STAI), which is divided into state (S-STAI) and trait (T-STAI) components, and two custom tests named ES3 and ES3-V [33]. The population data and test results are shown in Table 1. All 79 participants were included in the validation of SCPPG's agreement with the reference. Following this, SCPPG's capability to assess stress reactivity was evaluated. For this evaluation, reactivity was compared to the reference, and the control and patient groups were separated. Subjects from the control group were matched with those from the patient group based on age, sex, and body mass index (BMI). A total of 22 pairs were matched: 5 pairs of men and 17 pairs of women. The complete experimental protocol, including participant recruitment, inclusion and exclusion criteria, and informed consent, was approved by the ethical committee of the Gobierno de Aragón (CEICA, PI20/430), and all participants signed an informed consent.

B. STRESS PROTOCOL

The protocol included: i) 5 minutes of Basal state; ii) a Trail Making Test (TMT); iii) a Stroop Test (ST); iv) and 5 minutes of Recovery. During the Basal stage, participants were instructed to relax with the help of an audio guide. Next, they performed a TMT, which started with a page of randomly placed numbers that participants had to trace in ascending order using the index finger of their dominant hand, without lifting it from the tablet. The second page consisted of a sequence of numbers and letters, alternating between the two (1-A-2-B-3-C, etc.). The ST involved three pages. The first page had the words "red," "green," and "blue" randomly arranged in black ink for participants to read. The second page displayed the colors (red, green, and blue inks) that participants had to name. The third page showed the same words written in mismatched ink colors, and participants had to identify the ink color instead of the word. The Recovery phase involved unguided relaxation immediately after the ST.

C. FILTERING AND ARTIFACT REMOVAL

The Reference PPG and the SCPPG are subjected to third-order Butterworth high-pass filtering at 0.3 Hz and low-pass filtering at 10 Hz, applied in a forward–backward manner to achieve zero-phase response. In order to reduce motion artifacts, which often affect SCPPG signals and lead to incorrect or missed pulse detections, an artifact detector is used. This detector sets upper and lower limits for the Hjorth parameters [34], [35], calculated from signal data within 4-second sliding windows with a 25% overlap. The Hjorth parameters are defined as:

$$\begin{aligned} Activity&: \mathcal{H}_0(m) = \bar{w}_0(m) \\ Mobility&: \mathcal{H}_1(m) = \sqrt{\frac{\bar{w}_2(m)}{\bar{w}_0(m)}} \\ Complexity&: \mathcal{H}_2(m) = \sqrt{\frac{\bar{w}_4(m)}{\bar{w}_2(m)} - \frac{\bar{w}_2(m)}{\bar{w}_0(m)}}, \end{aligned} \tag{1}$$

where $\bar{w}_i$ represents the i-th order spectral moment. $\bar{w}_i$ is estimated using the temporal expression of the moments in the m-th window of P samples:

$$\hat{\bar{w}}_i(m) \approx \frac{2\pi}{P} \sum_{n=(m-1)P+1}^{mP} (x^{i/2}(n))^2, \tag{2}$$

being $x(n)$ either the Reference or the SCPPG, and P the number of samples corresponding to 4 seconds, *i.e.*, 1000 samples. For each parameter, the windowed series was smoothed with a 15-sample moving median and allowed the following upper and lower limits from this median: $-5/+3$ for $\mathcal{H}_0$, $-2/+2$ for $\mathcal{H}_1$, and $-0.8/+1$ for $\mathcal{H}_2$. Windows in which any parameter fell outside its allowed range were flagged as artifacts and discarded from further pulse detection.

Both SCPPG and Reference signals were analyzed in arbitrary units (a.u.), as their amplitudes depend on device-specific factors such as light intensity, camera sensitivity, and finger pressure, as well as on individual optical tissue properties. Although these factors prevent absolute calibration, they do not affect the relative waveform dynamics or variability metrics, which are the basis for the subsequent analysis.

D. PULSE DETECTION

Pulses are identified using the adaptive threshold algorithm described in [36]. This algorithm acquires the event series (t_k), which represents the timestamps of pulse occurrences at their maximum upslope. The following parameters were used: $\alpha = 0.3$ (fraction that sets the lower bound of the adaptive threshold relative to its current maximum); refractory period = 300 ms (interval after each detection during which additional detections are suppressed and the threshold is held constant); $\tau_{RR} = 0.4$ (fraction of the estimated pulse interval over which the threshold decays from its maximum to its minimum to adapt to rate changes); and low-pass-differentiator filter transition band from 4.4 Hz to 4.5 Hz. Parameter optimization was performed manually based on visual assessment of the data. Before performing PRV analysis, it is essential to identify and rectify any misdetection. To achieve this, the pulse-to-pulse interval series are calculated using the interval function $d_{IF}(t)$, defined as

$$d_{IF}(t) = \sum_k (t_k - t_{k-1})\delta(t - t_k), \tag{3}$$

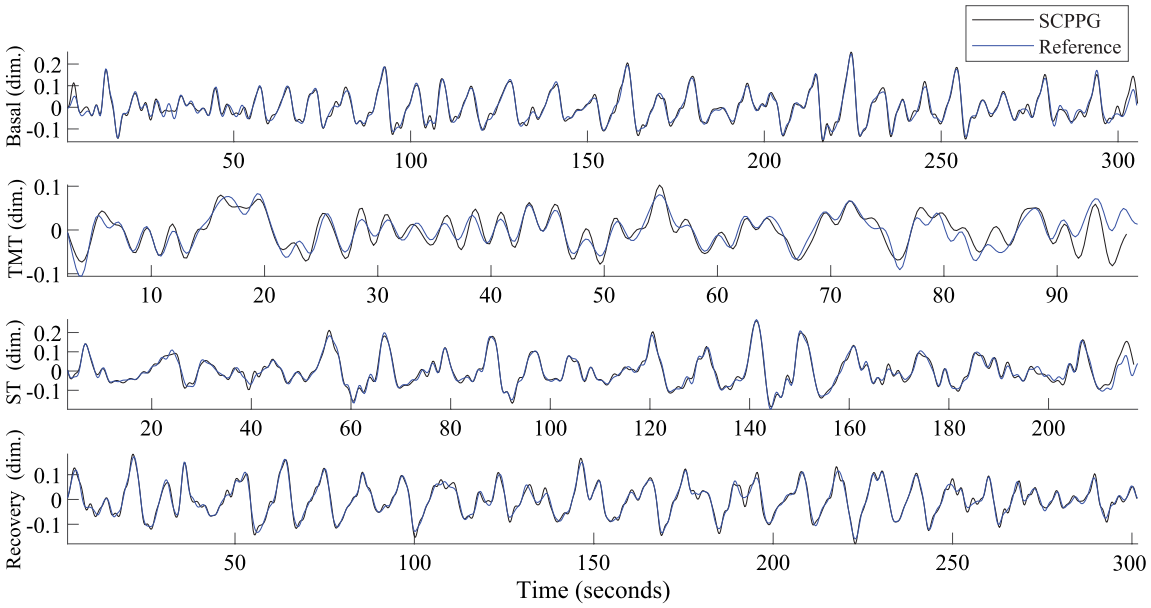

FIGURE 2. SCPPG (black) and reference (blue) modulating signals $m(t)$, expressed in dimensionless units (dim.), obtained with the IPFM model for each stage.

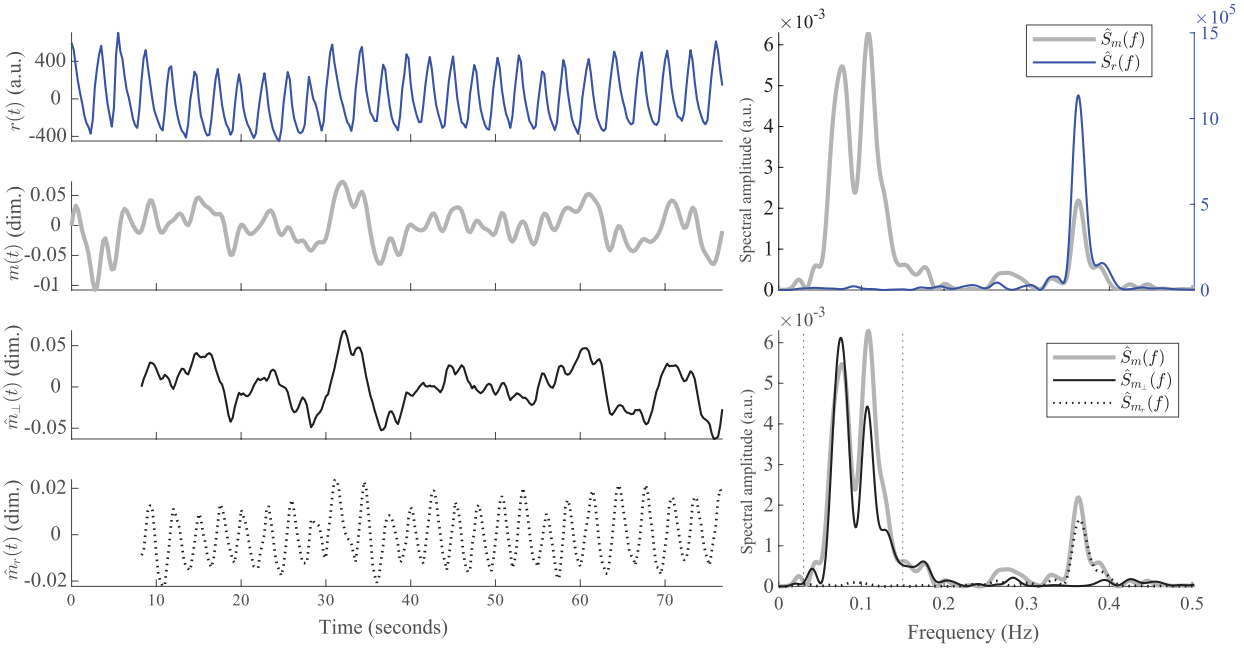

FIGURE 3. OSP decomposition. Respiratory rate outside LF band. *Left side top to bottom*: respiratory signal, modulation of the heart rate, modulation linearly related with respiration, residual component. *Right side top*: respiratory signal (blue) and modulation of the heart rate (gray) spectra. *Right side bottom*: modulation of the heart rate (gray), modulation linearly related with respiration (black) and residual component (dotted) spectra.

where k denotes the pulse index. Each event that occurs in time t_k is represented by a unit impulse function $\delta(t - t_k)$ scaled by the length of the preceding interval. False positives produce an abrupt shortening of this scaling due to the introduction of an additional spurious pulse between two actual pulses. A moving median of 30 samples is used to detect these outliers. The moving median produces an expected pulse-to-pulse interval (d_{EPPI}) at each t_k:

$$d_{EPPI}(t_k) = med\{d_{IF}(t_i)\};\ i \in [k-14, \cdots, k+15]. \quad (4)$$

The interval at t_k is considered a false positive if $d_{IF}(t_k) < (0.7 \times d_{EPPI}(tk))$. These false positives are removed from the t_k series, and $d_{IF}(t_k)$ is computed again. Next, the intervals at t_k are considered false negatives

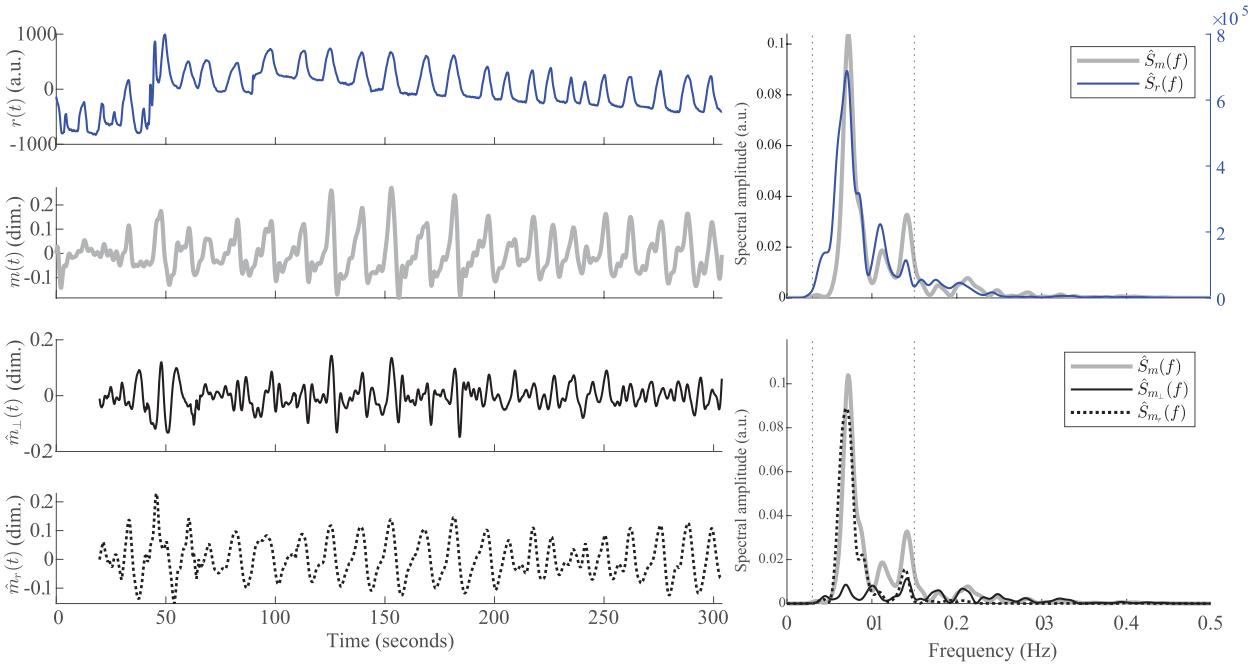

FIGURE 4. OSP decomposition. Respiratory rate within LF band. ***Left side top to bottom***: respiratory signal, modulation of the heart rate, modulation linearly related with respiration, residual component. ***Right side top***: respiratory signal (blue) and modulation of the heart rate (gray) spectra. ***Right side bottom***: modulation of the heart rate (gray), modulation linearly related with respiration (black) and residual component (dotted) spectra.

if $d_{IF}(t_k) > (1.3 \times d_{EPPI}(t_k))$. The treatment of false negatives is not the same for all PRV metrics, following the recommendations of [37]. This treatment is detailed in Section II-E.

E. PRV METRICS

Three time-domain and three frequency-domain metrics were calculated. The metrics in the time domain were the mean heart rate (MHR), the standard deviation of the normal-to-normal interval (SDNN), and the root mean square of successive differences (RMSSD) [38]. Based on [37], gap filling of false negatives is not recommended for these metrics. Therefore, they were calculated from $d_{IF}(t_k)$, excluding outliers in the t_k series.

Regarding frequency-domain metrics, an exploratory analysis revealed that respiratory frequency often fell within the low-frequency (LF) range, *i.e.*, 0.04 to 0.14 Hz, prompting an improved analysis of HRV metrics based on Orthogonal Subspace Projection (OSP) [29], [39]. The heart rate modulating signal, $m(t)$, which is presumed to carry information from the ANS, is calculated at 4 Hz using the time-varying integral pulse frequency modulation (IPFM) model [39] (see Figure 2). $m(t)$ is decomposed by the respiratory signal, $r(t)$, into a respiration-related linear component, $\hat{m}_r(t)$, and a residual component, $\hat{m}_\perp(t)$, containing other modulators. $\hat{m}_r(t)$ and $\hat{m}_\perp(t)$ are detrended with a 4th order Butterworth high-pass filter with a cutoff frequency of 0.03 Hz. Subsequently, the spectral densities $\hat{S}_{m_r}(f)$ and $\hat{S}_{m_\perp}(f)$ are estimated using Welch periodograms with 120-second Hamming windows and 30-second overlap within all available data in each phase of the protocol.

Spectral powers $P_{r,\mathrm{LF+HF}}$, representing the parasympathetic nervous system, and $P_{\perp,\mathrm{LF}}$, representing the sympathetic, are calculated by integrating $\hat{S}_{m_r}(f)$ and $\hat{S}_{m_\perp}(f)$ over 0.04-F_{max} Hz and 0.04-0.15 Hz, respectively, using trapezoidal numerical integration. F_{max} is the upper limit of the spectrum, computed as half of the MHR, which could be seen as the Nyquist criterion since the heart rate is sampled beat-to-beat. Figures 3 and 4 illustrate the OSP decomposition of $m(t)$, presenting one scenario where the respiratory rate exceeds the LF range and another where it is within the LF range. Observe that the former scenario is expected to yield results comparable to the conventional LF and high-frequency (HF) ranges, whereas the latter scenario results in significantly different outcomes.

Sympathovagal balance $\mathcal{R}'$ was computed as

$$\mathcal{R}' = \frac{P_{\perp,\mathrm{LF}}}{P_{r,\mathrm{LF+HF}} + P_{\perp,\mathrm{LF}}} \tag{5}$$

For a more detailed explanation of the chosen frequency-domain metrics, refer to [39]. The gaps detected in the t_k series were filled by an algorithm based on piecewise cubic Hermite interpolating polynomials [37] before computing the metrics in the frequency domain.

Then, the metrics are evaluated for physiological verosimilitude. The permissible ranges for these metrics are set at [40,180] bpm for MHR; [5,140] ms for SDNN and RMSSD; [0,0.003] *a.u.* for $P_{\perp,\mathrm{LF}}$; and [0,0.05] *a.u.* for $P_{r,\mathrm{LF+HF}}$. These ranges were derived from the highest and

TABLE 2. PRV metrics median and standard deviation, error median and standard deviation, Pearson correlation coefficient, number of missing cases, and bland-altman mean difference. All subjects.

	Values, *Median (SD)*	Error, *Median (SD)*	Pearson's r	Bland-Altman's Δ, *M [C.I.]* (%)	Missing, *N (%)*
MHR [bpm]					
Basal	72 (11)	0.0 (0.1)	1.00	0.0 [-0.2 0.3]	0 (0%)
TMT	77 (13)	0.0 (0.1)	1.00	0.0 [-0.3 0.3]	0 (0%)
ST	80 (15)	0.1 (0.2)	1.00	0.0 [-0.6 0.6]	1 (1.3%)
Recovery	71 (10)	0.0 (0.0)	1.00	0.0 [-0.1 0.2]	0 (0%)
SDNN [ms]					
Basal	66 (26)	1.0 (1.0)	1.00	2.1 [-4.5 8.8]	0 (0%)
TMT	50 (17)	1.5 (1.5)	0.99	3.4 [-6.6 13.4]	1 (1.3%)
ST	57 (19)	1.7 (2.6)	0.99	4.3 [-10.5 19.0]	1 (1.3%)
Recovery	61 (26)	1.0 (1.0)	1.00	2.3 [-3.2 7.8]	0 (0%)
RMSSD [ms]					
Basal	46 (20)	3.8 (3.2)	0.99	13.6 [-18.3 45.4]	2 (2.5%)
TMT	38 (13)	5.5 (5.3)	0.89	19.9 [-18.7 58.4]	0 (0%)
ST	41 (14)	6.1 (6.1)	0.90	21.2 [-16.4 58.8]	1 (1.3%)
Recovery	43 (21)	4.4 (3.6)	0.99	15.1 [-18.0 48.1]	1 (1.3%)
$P_{\perp,LF}$ $[a.u.]$					
Basal	42 (46) $\times 10^{-5}$	1 (8) $\times 10^{-5}$	0.98	1.4 [-17.7 20.4]	2 (2.5%)
TMT	29 (34) $\times 10^{-5}$	1 (2) $\times 10^{-5}$	1.00	3.8 [-21.9 29.6]	18 (22.8%)
ST	52 (44) $\times 10^{-5}$	2 (13) $\times 10^{-5}$	0.95	3.1 [-40.6 46.7]	5 (6.4%)
Recovery	47 (49) $\times 10^{-5}$	2 (10) $\times 10^{-5}$	0.98	2.1 [-22.1 26.4]	1 (1.3%)
$P_{r,LF+HF}$ $[a.u.]$					
Basal	164 (238) $\times 10^{-5}$	4 (19) $\times 10^{-5}$	1.00	0.7 [-14.8 16.3]	0 (0%)
TMT	31 (48) $\times 10^{-5}$	2 (3) $\times 10^{-5}$	1.00	7.5 [-34.9 49.8]	18 (22.8%)
ST	84 (79) $\times 10^{-5}$	3 (14) $\times 10^{-5}$	0.98	0.0 [-27.3 27.3]	5 (6.4%)
Recovery	92 (228) $\times 10^{-5}$	4 (15) $\times 10^{-5}$	1.00	-0.3 [-21.8 21.2]	0 (0%)

lowest values observed with the Reference, including ample allowance. Any metrics that fall outside the specified ranges are identified and removed from the agreement and reactivity analysis. Instead, the count of these cases is presented in Section III.

F. STATISTICAL ANALYSIS

PRV metrics derived from the SCPPG are compared to those from the Reference. The Pearson correlation is evaluated (r) with a significance threshold of $\alpha = 0.05$. Bland-Altman's mean difference (Δ), given as a percentage with its 95% confidence interval, is used to assess bias. To determine if the reactivity of controls and patients comes from probability distributions with different medians, a Wilcoxon rank sum test is conducted assuming nonnormal distributions. This assumption is supported by the presence of both normal and nonnormal distributions across different stages, as determined by a Shapiro-Wilk test. Although subjects in the control and patient groups are matched, as detailed in Section II-A, the statistical test is unpaired, as the primary estimand was the marginal between-group difference rather than within-pair contrasts. The effect size of the reactivity is measured using Cliff's Delta [40].

G. SOFTWARE AND APP AVAILABILITY

The smartphone acquisition app *BSICoS* used in this work is available on Google Play and on the Apple App Store. Android package: com.bsicos.bsicos_app. App Store ID: 6746410527. The app uses our open-source *scppg* library, available at pub.dev/scppg [41].

III. RESULTS

A. AGREEMENT

Table 3 presents the percentages of artifact-free time as determined by the Hjorth-based automatic detector. The stability of the SCPPG is demonstrated with 98.8% of the time being artifact-free, which is only 0.7% lower than the Reference value. Across different stages, no significant differences are observed, with a decrease of only 2.4% between the Basal and ST stages, representing the maximum and minimum values, respectively. The minimum value in the Reference is also observed in the ST stage, though it is only 1.2% lower than the Basal value.

The PRV values, along with the corresponding absolute errors, Pearson correlation coefficients, and the bias relative to the Reference, are presented in Table 2. The last column

TABLE 3. Percentage of artifact-free time according to Hjorth-based automatic detection.

	SCPPG (%)	Reference (%)
Basal	99.5	99.9
TMT	99.4	99.3
ST	97.1	98.7
Recovery	99.0	99.8
Total	**98.8**	**99.5**

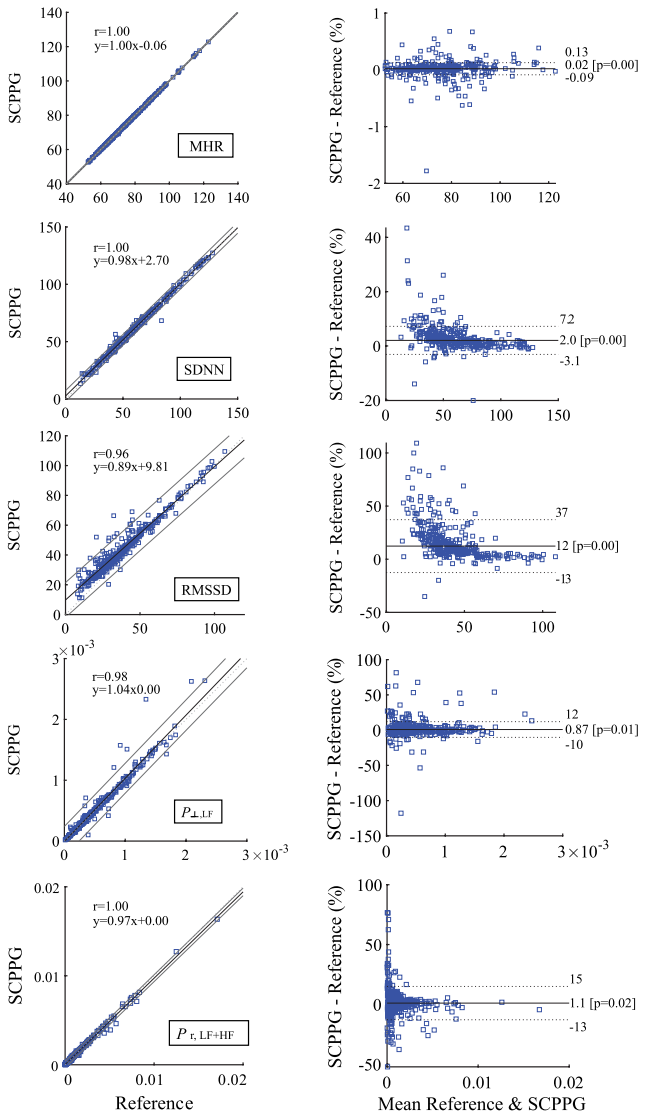

FIGURE 5. **Regression and bland-altman plots of relative differences for each metric. All stages together. *First*: MHR. *Second*: SDNN. *Third*: RMSSD. *Fourth*: $P_{\perp,LF}$. *Fifth*: $P_{r,LF+HF}$.**

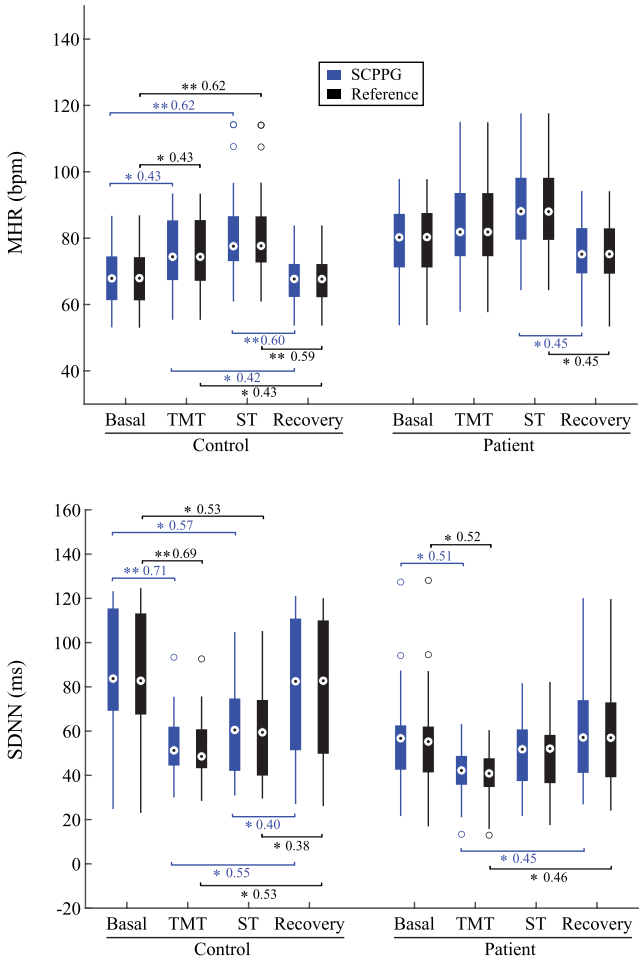

FIGURE 6. **Boxplots for each metric. Significant differences are marked with asterisks: * for $p < 0.05$ and ** for $p < 0.001$. Values after asterisks indicate the effect size. *Top*: MHR. *Bottom*: SDNN.**

represents the number of missing values. The errors are at least an order of magnitude smaller than the values of the metrics. Notably, the MHR error is exceptionally small, with an error magnitude three orders smaller than the metric value. All metrics exhibit high correlation, with coefficients exceeding 0.98, except for the RMSSD at the TMT stage, where the correlation is still substantial at 0.89. The p-values for all correlation tests were less than 0.001.

The number of missing values results from both the restrictions in the allowable range (see Section II-E), indicating a failure in the calculation, and the requirement of a minimum duration of 60 seconds for spectrum computation in frequency-domain metrics. For the time-domain metrics, the instances of unreliable measurements are less than 2.5%. In contrast, frequency-domain metrics display higher percentages of missing values, with the TMT stage reaching up to 22.8%. Excluding the TMT stage, the percentage of missing cases is less than 6.4%.

The bias is nearly negligible across all metrics except for RMSSD. This particular metric shows a steady positive bias in all phases, ranging from 13.6% to 21.2%.

Figure 5 presents the linear regressions and Bland-Altman plots for all combined stages. Every correlation has a p-value below 0.001, with the lowest correlation being 0.96. Once more, only the RMSSD exhibits a significant bias, though the overall effect of the stages diminishes this bias to 12%.

B. STRESS REACTIVITY

Figures 6 and 7 illustrate the distributions of PRV metrics across different stages for both control and patient groups. In the control group, increases in MHR and $\mathcal{R}'$ are observed during stress phases (TMT and ST) compared to relaxation phases (Basal and Recovery). Conversely, SDNN and RMSSD exhibit a decreasing trend. Significant differences and effect sizes are indicated in the graphs. Notably, significant differences were found in all metrics between the Basal stage and the two stress tests in the control

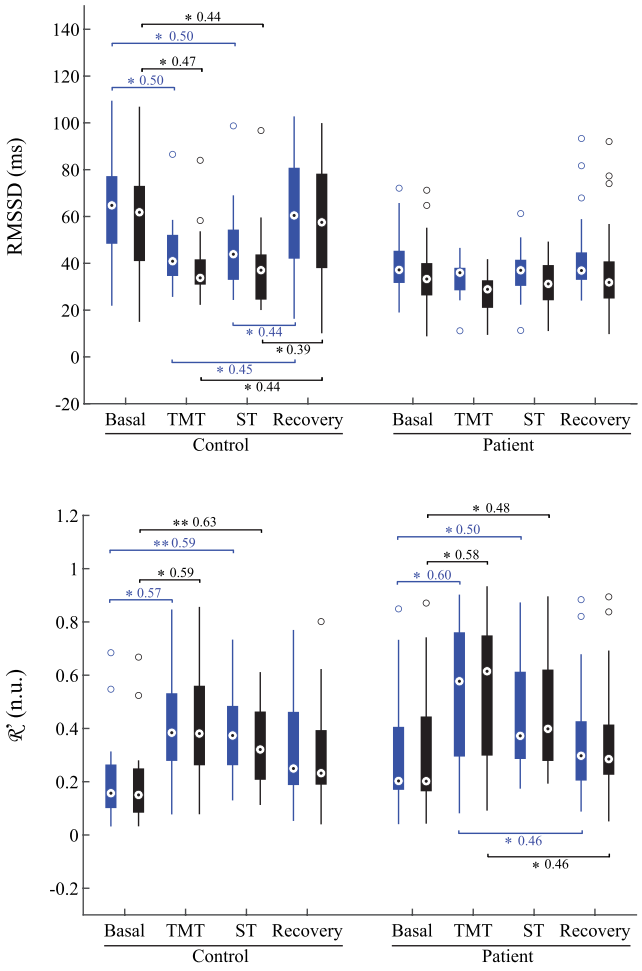

FIGURE 7. **Boxplots for each metric. Significant differences are marked with asterisks: * for $p < 0.05$ and ** for $p < 0.001$. Values after asterisks indicate the effect size. *Top*: RMSSD. *Bottom*: $\mathcal{R}'$.**

group. Additionally, significant differences are present in MHR, SDNN, and RMSSD between the stress tests and the Recovery phase.

In the patient group, reduced stress reactivity is observed. No significant differences are found between the Basal stage and the stress tests in MHR or RMSSD. However, differences in SDNN between Basal and TMT are observed, although with a reduced effect size (from 0.71 to 0.51). Significant differences are also noted in $\mathcal{R}'$ between Basal and both stress tests, with a smaller effect size between Basal and ST. The differences in MHR, RMSSD, and SDNN between the stress tests and the Recovery phase are either not significant or have reduced effect sizes. An exception is found in $\mathcal{R}'$, where differences are more pronounced in the patient group due to a significant increase during the TMT.

There is a high degree of agreement between the distributions obtained from the SCPPG and the Reference. The statistical tests for both the SCPPG and the Reference show consistent results in terms of statistical significance and effect size when there is good agreement.

The control group completed the TMT in 106±30 seconds, while the patient group took 118 ± 32 seconds. For the ST, the control group finished in 211 ± 31 seconds, compared to 233 ± 57 seconds for the patient group. The differences in median test durations between the groups are not statistically significant ($p = 0.25$ and $p = 0.33$).

IV. DISCUSSION

A. SCPPG FOR PRV MONITORING

Although quantitative indices such as correlation, bias, and absolute errors provide a descriptive view of agreement, their interpretation must be framed within the context of use. In this study, agreement was not assessed as an end but to evaluate whether SCPPG-derived metrics maintain the physiological variability required for stress assessment. Therefore, bias and absolute error were considered the main indicators of metrological correspondence, while correlation was interpreted as a complementary descriptor of rank-consistency across the measurement range. In combination, these metrics demonstrate a coherent level of agreement that supports the reliability of SCPPG for stress-monitoring applications. Overall, the agreement results should therefore be interpreted considering the intended application, emphasizing functional consistency in stress assessment over strict numerical equivalence.

The concordance between the PRV metrics derived from the SCPPG and the reference is exceptionally high. Notably, a correlation exceeding 0.96 ($p < 0.001$) indicates that the smartphone is as reliable as a commercial pulse oximeter, with correctable bias. The capability of the metrics obtained from the SCPPG to identify stress reactivity matches that of the reference device in terms of both statistical significance and effect size. Furthermore, the observed differences in reactivity between the control and patient groups support the use of the SCPPG for monitoring stress reactivity in the context of anxiety and depression assessments. The difference between stress stages and the Recovery was lower in subjects from the patient group, which is in agreement with the results found in [8]. The study of impaired recovery is highly intriguing, as research has connected it to a heightened risk factor for cardiovascular disease [8], [42]. Differential resting levels are evident between the patient and control groups. This is in agreement with the literature and may be a valuable measure, especially in longitudinal studies, given its relationship to the regulation of emotions and attention in addition to physiological regulation [2].

The overestimation of RMSSD may be attributed to the low sampling rate of SCPPG as lower sampling rates are more susceptible to noise, leading to signal distortion and reduced temporal resolution. Choi et al. [43] note that RMSSD requires a higher sampling frequency for robustness, unlike MHR, which averages out variability and remains robust. They recommend a minimum sampling frequency of 25 Hz. Similarly, Beres et al. [44] suggest that RMSSD demands higher sampling rates compared to metrics like MHR and

SDNN, reducing the necessary rate to 20 Hz. Thus, the camera's 24 Hz sampling rate is marginal or potentially insufficient, especially given Android's inconsistent handling of the camera, leading to lower sampling rates. Therefore, future research will explore higher sampling frequencies, supported by newer devices, and non-Android platforms for more stable sampling rates [45]. The positive bias observed in RMSSD does not compromise its interpretability. The bias remains relatively constant across phases, can be corrected post-hoc if required, and does not mask the phase-dependent differences relevant to stress reactivity. This suggests that the bias does not affect the metric's capacity to reflect autonomic modulation during stress.

Frequency domain metrics are derived through the integration of power spectral density estimates, which are calculated using Welch's method. The durations of the TMT and ST stages are notably shorter compared to those of the Basal and Recovery stages. Specifically, the TMT stage lasted an average of 109 seconds, with a range from 61 to 186 seconds. The ST stage had an average duration of 223 seconds, ranging from 153 to 368 seconds. Consequently, the number of segments available for Welch averaging is reduced in the shorter stages, resulting in increased variance. Additionally, the brief duration of the TMT stage often leads to a high number of missing cases in frequency domain metrics because it frequently does not meet the minimum requirement of 60 seconds necessary for spectrum calculation. It is important to highlight that although the test may exceed the minimum required duration, artifacts and misdetections can reduce the length of the valid signal used for metric computation, as gaps exceeding 10 seconds are prohibited. When larger gaps are present, the algorithm retains the longest segment without 10-second gaps [37]. The significant increase in $\mathcal{R}'$ observed during the TMT in the patient group might be attributed to the reduction in the number of cases. Although the metrics in the frequency domain are comparable to those in the time domain in terms of both correlation and error, a frequency domain metric could not be obtained in nearly a quarter of the TMT stages. For future applications, methods to lengthen the test duration should be investigated to guarantee sufficient data for reliable spectral estimation. It is noteworthy that only in one instance, the unique missing case in the Recovery stage, the Reference was able to obtain the metric where the SCPPG could not. In all other cases where the SCPPG failed, the Reference also failed. When using frequency domain metrics, it must be considered that they have more restrictive requirements and that the duration of the test is a crucial factor. Significant differences in HF and LF/HF ratio, calculated without OSP, are reported in the literatures [1] and [46]. To our knowledge, this study represents the first application of $\mathcal{R}'$ in the surveillance of stress reactivity, overcoming limitations in the respiratory rate.

One of the primary challenges in SCPPG is the significant exposure to the relative movement of the finger in relation to the camera. This problem is particularly detrimental to patients with tremors, even if the tremors are minor. Three subjects had tremors incompatible with the SCPPG recording. This represents 3.7% of the studied population. The sample is small to extrapolate this percentage to the general population, but it represents an important problem to be solved in the automation of monitoring. Using clamp-type sensors, similar to those used in clinical settings, connected to the smartphone would negate the main advantage of this system, which is the widespread availability of sensors in people's pockets. During the recording sessions, participants had to hold the smartphone in the same hand that had a pulse oximeter on the ring finger, leading to an uncomfortable and awkward grip. It is anticipated that the signal quality would be better if the free hand were used.

It is noteworthy the percentage of time and cases in which metrics can be obtained. Setting aside subjects excluded due to difficulties in remaining still, the percentage of artifact-free time is 98.78%, comparable to the Reference. This percentage is very high considering that hand movements are clearly transferred to the signal. It is likely that this percentage is mediated by a protocol design that allows for comfortably maintaining a stable position. The relaxation stages are performed in complete stillness, and the ST is a spoken task. The only stage that demands movement is the TMT. This test was conducted with the dominant hand while holding the smartphone with the non-dominant hand. This independence contributed to the stability of the recording. When designing other stress-inducing tasks, particularly those that involve interacting with the recording device - centralizing all interactions on a single device is an ideal scenario-, it is recommended to consider that such interaction might introduce artifacts. This matter is presently under investigation. The stage with the highest number of artifacts was the ST. This was also the stage where subjects reported the highest stress. This, combined with the longer duration of the test and the consequent fatigue, suggests that the induced stress level is more determinant for the quality of the signals than the manner of interacting with the device. An interesting line of work involves the interplay between human-device interaction design and stress-inducing tasks that facilitate functionality. It should be noted that artifact-free time has been measured with an automatic detector. This does not imply that the non-rejected segments have a good signal-to-noise ratio nor that the detections are error-free. The Hjorth-based detector rejects segments with energy peaks and those presenting high complexity, that is, segments with a relatively wide frequency spectrum. The steps of correcting errors and discarding values that fall outside of reasonable ranges are essential for achieving reliable measurements.

B. STRESS REACTIVITY

The nature of the stressor, although not studied in this work, appears to significantly influence stress reactivity.

In the study by Hu et al. [17], individuals with depression exhibited hyperreactivity when subjected to a stressor in the form of an interview, whereas hyporeactivity was observed during a cognitively challenging task. It was suggested by the authors that individuals suffering from depression might demonstrate reduced motivation to achieve positive outcomes in tasks requiring cognitive effort. Conversely, their response to emotional distress experienced in daily life, such as that induced by interviews, may be heightened. Studies reviewed by Kibler and Ma [18] also demonstrated an increase in reactivity during speech tasks. Based on this hypothesis, the hyporeactivity observed in both the ST and the TMT was anticipated. Furthermore, as noted by Salomon et al. [47], diminished cardiovascular response and compromised recovery in individuals with current major depression could be influenced by their mood state. This primarily indicates deficiencies in motivation rather than physiological abnormalities within the cardiovascular system.

Although the distributions of the metrics differ between patient and control groups, the variability between subjects is substantial. Therefore, establishing thresholds to determine whether the reactivity corresponds to a healthy or diseased nervous system does not appear to be the optimal approach. Instead, the trend of reactivity should be examined in subsequent measurements. An increase in reactivity during treatment would suggest an improvement in mental health. To evaluate the feasibility and effectiveness of this follow-up, a longitudinal study is required. Specifically, it is crucial to investigate the effects of performing stressor tests recurrently. As patients become accustomed to these tasks, they may exhibit decreased interest in optimal performance, resulting in reduced stress levels. Additionally, an enhanced ability to complete tasks may contribute to reduced stress. Investigating the variations in habituation between individuals with and without depression could be a compelling area of research. This is particularly pertinent given the theory that decreased engagement in cognitively demanding activities underlies the blunted stress response observed in individuals with depression [17]. Furthermore, Brindle et al. [10] suggested that stress reactivity is mediated by stress experience rather than stress exposure. Including test scores as an additional metric could provide valuable insights into the patients' commitment to the tasks.

Although PRV is not identical to HRV due to the inclusion of electromechanical delay, vascular timing (pre-ejection period, pulse transit time), and fiducial differences in PPG, the literature supports PRV as a surrogate of HRV [22], while anticipating larger discrepancies for short-lag metrics such as RMSSD. In the context of stress reactivity, this difference could be not detrimental: sympathetic vasoconstriction, blood pressure changes and transient increases in arterial stiffness are integral components of the autonomic stress response and modulate PRV. Thus, PRV provides additional physiologically relevant information that may be advantageous in this application.

The effects of anxiety are difficult to remove and the comorbidity of anxiety and depression is frequent. Numerous studies have observed the inclusion of patients with both depression and anxiety, complicating the attribution of effects solely to depression. Instead, these effects may be attributed to the broader spectrum of anxiety and depression [3]. Several reports in the literature have not identified significant differences when comparing groups with depression and anxiety, either in stress reactivity [7], [17] or in basal levels [7]. Conversely, other studies have yielded different findings. For instance, [48] reported that HF power levels were elevated in patients with comorbid MDD and GAD compared to those with only GAD. Additionally, an investigation that examined skin conductance, skin temperature, pupil diameter, and heart rate in participants exposed to unpleasant, pleasant, and neutral images indicated that anxiety and depression influence autonomic output reactivity differently. This distinction may aid in differentiating individuals with anxiety from those with depression [49]. Furthermore, in [12], individuals with generalized anxiety disorder exhibited reduced reactivity compared to the control group, while those with social anxiety disorder demonstrated increased reactivity. The incorporation of objective measures, such as HRV, in longitudinal investigations of these conditions could enhance the understanding of their interconnections and distinctions [50].

Two patients reported benzodiazepine use. To assess potential confounding, a sensitivity analysis was performed excluding the two corresponding patient-control pairs. All previously significant contrasts remained significant, no non-significant contrast became significant, and effect sizes changed only marginally ($|\Delta| \leq 0.1$). Due to the limited number of benzodiazepine cases, these findings should be approached with caution and are insufficient for making subgroup inferences. Larger sample sizes are necessary to elucidate the effects of benzodiazepines on baseline levels and stress reactivity. With respect to non-tricyclic antidepressants, Hu et al. [17] demonstrated that although antidepressant medication affects baseline levels, it does not influence stress reactivity.

PPG morphological metrics have been employed to evaluate stress responses, demonstrating distinct differences between individuals with depression and those who are healthy [13]. It is recommended that future research investigate whether similar assessments can be conducted using SCPPG.

C. LIMITATIONS

Differences in stress reactivity between men and women have been documented. Additionally, variations in women depending on the menstrual cycle phase have been noted [3]. In this study, the groups were matched by sex, though the menstrual phase was not accounted for.

The study utilized a single smartphone model, the Xiaomi Pocophone F1, released in 2018, which limits the

ability to generalize findings to newer devices. However, most modern smartphones are equipped with cameras and sensors that offer superior optical capabilities. Therefore, hardware performance is unlikely to be a significant constraint. Instead, future evaluations should concentrate on examining the efficacy of various devices in measuring stress reactivity using the proposed or similar protocols, rather than focusing on HRV agreement without contextual application. In addition, camera resolution is not a critical factor for PRV estimation. SCPPG signals are obtained by spatially averaging the green channel over the entire frame, which suppresses sensor noise and makes the method robust even at low resolutions. In this study, a resolution of 320×240 pixels was used. Higher resolutions do not provide additional physiological information for PRV since temporal sampling, and not spatial detail, is the limiting factor.

It should be noted that the validation was performed on participants able to maintain finger stability, excluding three cases (3.7%) affected by tremor. While this ensures comparable signal quality between SCPPG and the reference, it also restricts the evaluation to users capable of holding the smartphone still. Importantly, this percentage likely reflects a lower bound of real-world failure rates, since tremor prevalence increases in older populations and may be exacerbated by anxiety, psychomotor agitation, or medication effects. As a result, SCPPG may systematically underperform in subgroups for whom stress monitoring is especially relevant, introducing potential selection bias and limiting usability in longitudinal deployment. Future developments should therefore focus on improving robustness—through enhanced signal-quality control, motion-aware pulse-timing extraction, and interaction designs that mitigate micro-movements to reduce the proportion of users for whom SCPPG becomes unusable.

The validation was performed under controlled laboratory conditions, where participants were instructed to remain seated and minimize movement. While this approach ensured signal stability and allowed for a reliable comparison with the reference device, it does not reflect the full range of situations expected in ambulatory monitoring. Therefore, the present results should be interpreted as representative of performance under stable conditions. Future studies should extend the validation to less controlled environments and naturalistic settings to evaluate the robustness of SCPPG during daily activities.

The analysis conducted assumes stationarity within each phase of the protocol, which may not hold true for all cases, particularly in the recovery phase performed immediately after the stressor. Significant differences may exist between the first and last minutes of this phase. Stress accumulation during the tests and relaxation during the basal phase could also impact results. Additional research and supporting evidence are needed to validate these assumptions and understand their implications.

The respiratory signal captured by a band was used for the decomposition of the modulating signal. In cases where only a smartphone is utilized, this respiratory signal must be extracted from the SCPPG. This process is complex and requires thorough investigation, as discussed in [51].

Additionally, the stress-inducing tasks were selected because their autonomic response and sensitivity to cognitive load are well established in the literature. However, it is not assumed that they are the most suitable for all contexts. In longitudinal studies, repeated exposure to the same tasks could lead to habituation and attenuated stress responses. Therefore, future work should evaluate alternative stressors or task designs to maintain their efficacy over repeated assessments.

Ultimately, depression measurements were not performed, preventing a correlation analysis with stress reactivity levels.

D. FUTURE LINES

Measurement robustness and physiological specificity will be enhanced, generalizability will be expanded, and clinical utility will be established through longitudinal assessment. Robustness to motion, illumination changes, and finger-pressure variability will be increased by integrating signal-quality control and artifact-resilient pulse-timing extraction. Autonomic contributions will be better isolated by explicitly accounting for respiratory influences when appropriate. To improve comparability across sessions, within-subject normalization that considers time-of-day and common behavioral or pharmacological confounders will be applied. In parallel, broader and more diverse cohorts (age, sex, skin tone, comorbidities) will be enrolled to characterize population-level variability and to derive more generalizable reference values for stress reactivity.

Longitudinal use will be evaluated to determine whether SCPPG-derived stress reactivity can track treatment progress over time and yield clinically meaningful change metrics suitable for routine follow-up. Practical measurement schedules for repeated assessments will be defined, and the types of stressors most informative in longitudinal settings will be identified while habituation is mitigated. Responses to real-world stressors will be examined so that the translation of laboratory findings to everyday contexts can be assessed.

Validation under real-world usage conditions will be further extended. Performance will be evaluated in parallel with continuous-monitoring wearables, and data collection will be carried out using each participant's own smartphone, thereby capturing heterogeneity in camera hardware and operating systems. Usability, adherence, and energy efficiency will be examined to refine acquisition workflows, and the implementation of on-device processing pipelines will be prioritized so that data transfer is minimized and privacy is maximized. In this regard, the first steps have already been

taken with the validation of a mobile application design [52], this time focused on use by patients, and the creation of a minimum viable product (MVP) desktop application for healthcare professionals [53].

V. CONCLUSION

The results of this study support the effectiveness of SCPPG technology in evaluating the stress response, making it suitable for monitoring depression and anxiety. The PRV metrics show a strong correlation ($r \geq 0.96$, $p < 0.001$) and minimal bias ($\Delta \leq 2\%$) for all metrics excluding RMSSD. While RMSSD presents some bias ($\Delta = 12\%$), it does not conceal the differences between patient and control groups, and the correlation remains significant ($r = 0.96$, $p < 0.001$). Consequently, this technology proves valuable for evaluating both baseline states and stress reactivity. One of the most promising applications of this technology involves investigating it within expanded longitudinal cohorts, particularly given the ubiquitous integration of smartphones in modern society.

ACKNOWLEDGMENT

Computations were performed by the ICTS NANBIOSIS (HPC Unit, University of Zaragoza).

REFERENCES

[1] J. Rottenberg, "Cardiac vagal control in depression: A critical analysis," *Biol. Psychol.*, vol. 74, no. 2, pp. 200–211, Feb. 2007.

[2] J. L. Hamilton and L. B. Alloy, "Atypical reactivity of heart rate variability to stress and depression across development: Systematic review of the literature and directions for future research," *Clin. Psychol. Rev.*, vol. 50, pp. 67–79, Dec. 2016.

[3] C. Schiweck, D. Piette, D. Berckmans, S. Claes, and E. Vrieze, "Heart rate and high frequency heart rate variability during stress as biomarker for clinical depression. A systematic review," *Psychol. Med.*, vol. 49, no. 2, pp. 200–211, Jan. 2019.

[4] R. Castaldo, P. Melillo, U. Bracale, M. Caserta, M. Triassi, and L. Pecchia, "Acute mental stress assessment via short term HRV analysis in healthy adults: A systematic review with meta-analysis," *Biomed. Signal Process. Control*, vol. 18, pp. 370–377, Apr. 2015.

[5] A. A. Campbell and B. E. Wisco, "Respiratory sinus arrhythmia reactivity in anxiety and posttraumatic stress disorder: A review of literature," *Clin. Psychol. Rev.*, vol. 87, Jul. 2021, Art. no. 102034.

[6] S. Cohen, D. Janicki-Deverts, and G. E. Miller, "Psychological stress and disease," *JAMA*, vol. 298, no. 14, p. 1685, 2007.

[7] K. Kircanski, C. E. Waugh, M. C. Camacho, and I. H. Gotlib, "Aberrant parasympathetic stress responsivity in pure and co-occurring major depressive disorder and generalized anxiety disorder," *J. Psychopathology Behav. Assessment*, vol. 38, no. 1, pp. 5–19, Mar. 2016.

[8] K. Salomon, A. Clift, M. Karlsdóttir, and J. Rottenberg, "Major depressive disorder is associated with attenuated cardiovascular reactivity and impaired recovery among those free of cardiovascular disease," *Health Psychol.*, vol. 28, no. 2, pp. 157–165, 2009.

[9] A. C. Phillips, K. Hunt, G. Der, and D. Carroll, "Blunted cardiac reactions to acute psychological stress predict symptoms of depression five years later: Evidence from a large community study," *Psychophysiology*, vol. 48, no. 1, pp. 142–148, Jan. 2011.

[10] R. C. Brindle, A. T. Ginty, and S. M. Conklin, "Is the association between depression and blunted cardiovascular stress reactions mediated by perceptions of stress?" *Int. J. Psychophysiology*, vol. 90, no. 1, pp. 66–72, 2013.

[11] A. J. Fisher and M. G. Newman, "Heart rate and autonomic response to stress after experimental induction of worry versus relaxation in healthy, high-worry, and generalized anxiety disorder individuals," *Biol. Psychol.*, vol. 93, no. 1, pp. 65–74, Apr. 2013.

[12] D. F. Tolin, E. Lee, H. C. Levy, A. Das, L. Mammo, B. W. Katz, and G. J. Diefenbach, "Psychophysiological assessment of stress reactivity and recovery in anxiety disorders," *J. Anxiety Disorders*, vol. 82, Aug. 2021, Art. no. 102426.

[13] S. Kontaxis, E. Gil, V. Marozas, J. Lázaro, E. García, M. Posadas-de Miguel, S. Siddi, M. L. Bernal, J. Aguiló, J. M. Haro, C. de la Cámara, P. Laguna, and R. Bailón, "Photoplethysmographic waveform analysis for autonomic reactivity assessment in depression," *IEEE Trans. Biomed. Eng.*, vol. 68, no. 4, pp. 1273–1281, Apr. 2021.

[14] D. Sheffield, R. Krittayaphong, W. E. Cascio, K. C. Light, R. N. Golden, J. B. Finkel, G. Glekas, G. G. Koch, and D. S. Sheps, "Heart rate variability at rest and during mental stress in patients with coronary artery disease: Differences in patients with high and low depression scores," *Int. J. Behav. Med.*, vol. 5, no. 1, pp. 31–47, Mar. 1998.

[15] E. W. Thornton and C. N. Hallas, "Affective status following myocardial infarction can predict long-term heart rate variability and blood pressure reactivity," *Brit. J. Health Psychol.*, vol. 4, no. 3, pp. 231–245, Sep. 1999.

[16] S. C. Matthews, R. A. Nelesen, and J. E. Dimsdale, "Depressive symptoms are associated with increased systemic vascular resistance to stress," *Psychosomatic Med.*, vol. 67, no. 4, pp. 509–513, 2005.

[17] M. X. Hu, F. Lamers, E. J. C. de Geus, and B. W. J. H. Penninx, "Differential autonomic nervous system reactivity in depression and anxiety during stress depending on type of stressor," *Psychosomatic Med.*, vol. 78, no. 5, pp. 562–572, 2016.

[18] J. L. Kibler and M. Ma, "Depressive symptoms and cardiovascular reactivity to laboratory behavioral stress," *Int. J. Behav. Med.*, vol. 11, no. 2, pp. 81–87, Jun. 2004.

[19] R. C. Kessler, "The effects of sressfull life events on depression," *Annu. Rev. Psychol.*, vol. 48, pp. 191–214, Feb. 1997.

[20] V. Krishnan and E. J. Nestler, "The molecular neurobiology of depression," *Nature*, vol. 455, no. 7215, pp. 894–902, 2008.

[21] M. Harris, N. Glozier, R. Ratnavadivel, and R. R. Grunstein, "Obstructive sleep apnea and depression," *Sleep Med. Rev.*, vol. 13, no. 6, pp. 437–444, Dec. 2009.

[22] E. Gil, M. Orini, R. Bailón, J. M. Vergara, L. Mainardi, and P. Laguna, "Photoplethysmography pulse rate variability as a surrogate measurement of heart rate variability during non-stationary conditions," *Physiological Meas.*, vol. 31, no. 9, pp. 1271–1290, Sep. 2010.

[23] M. Shabaan, K. Arshid, M. Yaqub, F. Jinchao, M. S. Zia, G. R. Bojja, M. Iftikhar, U. Ghani, L. S. Ambati, and R. Munir, "Survey: Smartphone-based assessment of cardiovascular diseases using ECG and PPG analysis," *BMC Med. Informat. Decis. Making*, vol. 20, no. 1, p. 177, Jul. 2020.

[24] C. G. Scully, J. Lee, J. Meyer, A. M. Gorbach, D. Granquist-Fraser, Y. Mendelson, and K. H. Chon, "Physiological parameter monitoring from optical recordings with a mobile phone," *IEEE Trans. Biomed. Eng.*, vol. 59, no. 2, pp. 303–306, Feb. 2012.

[25] D. J. Plews, B. Scott, M. Altini, M. Wood, A. E. Kilding, and P. B. Laursen, "Comparison of heart-rate-variability recording with smartphone photoplethysmography, polar H7 chest strap, and electrocardiography," *Int. J. Sports Physiol. Perform.*, vol. 12, no. 10, pp. 1324–1328, Nov. 2017.

[26] I. Liu, S. Ni, and K. Peng, "Happiness at your fingertips: Assessing mental health with smartphone photoplethysmogram-based heart rate variability analysis," *Telemedicine E-Health*, vol. 26, no. 12, pp. 1483–1491, Dec. 2020.

[27] L. Dall'Olio, N. Curti, D. Remondini, Y. Safi Harb, F. W. Asselbergs, G. Castellani, and H.-W. Uh, "Prediction of vascular aging based on smartphone acquired PPG signals," *Sci. Rep.*, vol. 10, no. 1, Nov. 2020.

[28] D. Cajal, M. P.-D. Miguel, C. de la Camara, S. Kontaxis, J. Lazaro, and R. Bailon, "Smartphone PPG validation for a depression assessment protocol," in *Proc. E-Health Bioeng. Conf. (EHB)*, Nov. 2022, pp. 1–4.

[29] C. Varon, J. Lázaro, J. Bolea, A. Hernando, J. Aguiló, E. Gil, S. Van Huffel, and R. Bailón, "Unconstrained estimation of HRV indices after removing respiratory influences from heart rate," *IEEE J. Biomed. Health Informat.*, vol. 23, no. 6, pp. 2386–2397, Nov. 2019.

[30] L. T. van Zyl, T. Hasegawa, and K. Nagata, "Effects of antidepressant treatment on heart rate variability in major depression: A quantitative review," *BioPsychoSocial Med.*, vol. 2, no. 1, p. 12, Dec. 2008.

[31] T.-C. Yeh, L.-C. Kao, N.-S. Tzeng, T. B. J. Kuo, S.-Y. Huang, C.-C. Chang, and H.-A. Chang, "Heart rate variability in major depressive disorder and after antidepressant treatment with agomelatine and paroxetine: Findings from the Taiwan study of depression and anxiety (TAISDA)," *Prog. Neuro-Psychopharmacology Biol. Psychiatry*, vol. 64, pp. 60–67, Jan. 2016.

[32] J. Davidson, L. Watkins, M. Owens, S. Krulewicz, K. Connor, D. Carpenter, R. Krishnan, and C. Nemeroff, "Effects of paroxetine and venlafaxine XR on heart rate variability in depression," *J. Clin. Psychopharmacology*, vol. 25, no. 5, pp. 480–484, 2005.

[33] J. Aguiló, P. Ferrer-Salvans, A. García-Rozo, A. Armario, A. Corbí, F. J. Cambra, R. Bailón, A. González-Marcos, G. Caja, S. Aguiló, R. López-Antón, A. Arza-Valdés, and J. M. Garzón-Rey, "Project ES3: Attempting to quantify and measure the level of stress," *Rev. Neurol.*, vol. 61, no. 9, pp. 405–415, 2015.

[34] E. Peralta, J. Lazaro, R. Bailon, V. Marozas, and E. Gil, "Optimal fiducial points for pulse rate variability analysis from forehead and finger photoplethysmographic signals," *Physiological Meas.*, vol. 40, no. 2, Feb. 2019, Art. no. 025007.

[35] B. Hjorth, "EEG analysis based on time domain properties," *Electroencephalogr. Clin. Neurophysiology*, vol. 29, no. 3, pp. 306–310, Sep. 1970.

[36] J. Lázaro, E. Gil, J. M. Vergara, and P. Laguna, "Pulse rate variability analysis for discrimination of sleep-apnea-related decreases in the amplitude fluctuations of pulse photoplethysmographic signal in children," *IEEE J. Biomed. Health Informat.*, vol. 18, no. 1, pp. 240–246, Jan. 2014.

[37] D. Cajal, D. Hernando, J. Lázaro, P. Laguna, E. Gil, and R. Bailón, "Effects of missing data on heart rate variability metrics," *Sensors*, vol. 22, no. 15, p. 5774, Aug. 2022.

[38] Task Force of the European Society of Cardiology and the North American Society of Pacing and Electrophysiology, "Heart rate variability: Standards of measurement, physiological interpretation, and clinical use," *Eur. Heart J.*, vol. 17, no. 3, pp. 354–381, 1996.

[39] L. Sörnmo, R. Bailón, and P. Laguna, "Spectral analysis of heart rate variability in time-varying conditions and in the presence of confounding factors," *IEEE Rev. Biomed. Eng.*, vol. 17, pp. 322–341, 2024.

[40] N. Cliff, "Dominance statistics: Ordinal analyses to answer ordinal questions," *Psychol. Bull.*, vol. 114, no. 3, pp. 494–509, 1993.

[41] D. Cajal, "SCPPG," Zenodo (CERN), Geneva, Switzerland, Tech. Rep. 15482223, 2025, doi: 10.5281/zenodo.15482223.

[42] J. L. H. Schuler and W. H. O'Brien, "Cardiovascular recovery from stress and hypertension risk factors: A meta-analytic review," *Psychophysiology*, vol. 34, no. 6, pp. 649–659, Nov. 1997.

[43] A. Choi and H. Shin, "Photoplethysmography sampling frequency: Pilot assessment of how low can we go to analyze pulse rate variability with reliability?" *Physiological Meas.*, vol. 38, no. 3, pp. 586–600, Mar. 2017.

[44] S. Béres and L. Hejjel, "The minimal sampling frequency of the photoplethysmogram for accurate pulse rate variability parameters in healthy volunteers," *Biomed. Signal Process. Control*, vol. 68, Jul. 2021, Art. no. 102589.

[45] G. Lovisotto, H. Turner, S. Eberz, and I. Martinovic, "Seeing red: PPG biometrics using smartphone cameras," in *Proc. IEEE/CVF Conf. Comput. Vis. Pattern Recognit. Workshops (CVPRW)*, Jun. 2020, pp. 3565–3574.

[46] A. H. Kemp, D. S. Quintana, M. A. Gray, K. L. Felmingham, K. Brown, and J. M. Gatt, "Impact of depression and antidepressant treatment on heart rate variability: A review and meta-analysis," *Biol. Psychiatry*, vol. 67, no. 11, pp. 1067–1074, Jun. 2010.

[47] K. Salomon, L. M. Bylsma, K. E. White, V. Panaite, and J. Rottenberg, "Is blunted cardiovascular reactivity in depression mood-state dependent? A comparison of major depressive disorder remitted depression and healthy controls," *Int. J. Psychophysiology*, vol. 90, no. 1, pp. 50–57, Oct. 2013.

[48] S. G. Hofmann, S. M. Schulz, S. Heering, F. Muench, and L. F. Bufka, "Psychophysiological correlates of generalized anxiety disorder with or without comorbid depression," *Int. J. Psychophysiology*, vol. 78, no. 1, pp. 35–41, Oct. 2010.

[49] L. De Zorzi, S. Ranfaing, J. Honoré, and H. Sequeira, "Autonomic reactivity to emotion: A marker of sub-clinical anxiety and depression symptoms?" *Psychophysiology*, vol. 58, no. 4, Apr. 2021, Art. no. e13774.

[50] T. E. Moffitt, A. Caspi, H. Harrington, B. J. Milne, M. Melchior, D. Goldberg, and R. Poulton, "Generalized anxiety disorder and depression: Childhood risk factors in a birth cohort followed to age 32," *Psychol. Med.*, vol. 37, no. 3, pp. 441–452, Mar. 2007.

[51] J. Lázaro, Y. Nam, E. Gil, P. Laguna, and K. H. Chon, "Respiratory rate derived from smartphone-camera-acquired pulse photoplethysmographic signals," *Physiological Meas.*, vol. 36, no. 11, pp. 2317–2333, Nov. 2015.

[52] E. Tausiet, T. Blanco, D. Cajal, Á. Marco, P. Aznar, and R. Bailón, "Digitalization of mental health tracking through a mobile app to monitor anxiety and depression: A design perspective," in *Proc. Int. Joint Conf. Mech., Design Eng. Adv. Manuf.*, 2025, pp. 631–640.

[53] T. Blanco, N. Carrera, D. Cajal, E. Gil, and R. Casas, "Visual Programming for Minimum Viable Product in a Health Design Project," in *Proc. Int. Joint Conf. Mech., Design Eng. Adv. Manuf.*, 2025, pp. 607–619.

DIEGO CAJAL received the B.Sc. degree in telecommunications technology engineering and the M.Sc. and Ph.D. degrees in biomedical engineering, in 2018, 2019, and 2025, respectively. He is currently a Ph.D. Researcher, who joined the BSICoS Group, in 2019. His research interests include wearable devices and biomedical signal processing, with a particular interest in heart rate variability analysis applied to areas, such as mental health and sleep apnea.

CONCEPCIÓN DE LA CÁMARA received the degree in medicine and surgery, in 1989, and the Ph.D. degree (cum laude), in 1999. After completing her residency in psychiatry at the University Clinical Hospital of Zaragoza, in 1994, with research stays in Liverpool and Rotterdam, she combined clinical practice with teaching and research. Since 2003, she has been an Assistant of Psychiatry at HCUZ and an Associate Professor at the Faculty of Medicine. From 2009 to 2019, she tutored Psychiatry residents with a strong emphasis on research. She is currently a Psychiatrist and an Associate Professor with the University of Zaragoza. Her research interests include psychogeriatrics and psychosomatics, with contributions to multicenter and collaborative projects. She leads the DGA Research Group of the Aragon Government, is part of the Liaison Psychiatry Group at IIS Aragón, and is a member of CIBERSAM.

MAR POSADAS-DE MIGUEL received the Licenciatura degree in psychology (clinical and health accreditation) from UNED and the master's degree in medical research from the University of Zaragoza. She is currently a Psychologist with experience in clinical practice, research, and academic publishing. She worked at the Aragon Health Research Institute (IIS Aragón), from 2014 to 2022, combining roles in psychology and research, and served as the Journal Manager for *The European Journal of Psychiatry*. She has also collaborated with organizations, such as Asociación de Trastornos Depresivos de Aragón (AFDA) and Kairós Cooperativa de Iniciativa Social.

NOEL TORRIJOS was the General Health Psychologist. He is currently the Head of the SOS Adolescentes Project. He has more than ten years of experience working with adolescents and young people as a Psychologist and as a Career and Educational Counselor for the Government of Aragón.

ÓSCAR NADAL was a Health Psychologist. He has been with the SOS Adolescentes Program, Interdiocesan Solidarity Center, Huesca, since May 2023. He also has one year of prior experience in family mediation and intervention.

TERESA BLANCO received the Ph.D. degree in design, manufacturing, and industrial project management from the Polytechnic University of Valencia. She has transdisciplinary training in the humanities, design engineering, and innovation. She is currently a Professor and a Researcher with the University of Zaragoza, where she is part of the Human OpenWare Research Group (HOWLab) within the Aragon Institute of Engineering Research (I3A). She has participated in numerous research and technology transfer projects, leading several of them, and has promoted two university spin-offs. Her current research interests include developing hybrid methodologies that integrate design and technology to create technological ecosystems and innovations oriented toward health and the one health approach.

SARA SIDDI received the Ph.D. degree. She is currently a Neuropsychologist with Parc Sanitari Sant Joan de Déu and a Postdoctoral Researcher with the Impact and Prevention of Severe Mental Disorders Group. She studies neurocognitive mechanisms in disorders, particularly depression, and applies advanced methods to interpret multidimensional data. She integrates clinical practice with research to enhance patient assessment and treatment, and currently coordinates EUPROMENS for the Spanish hub, a project aimed at professional training and exchange across Europe, with the goal of strengthening mental health care through multidisciplinary collaboration.

PABLO ARMAÑAC received the B.Sc. degree in electronics and automation engineering, the M.Sc. degree in biomedical engineering, and the Ph.D. degree in biomedical engineering from the Aragon Engineering Research Institute, University of Zaragoza, Zaragoza, Spain, in 2017, 2018, and 2024, respectively. He joined the BSICoS Group, in 2018, where he is currently a Ph.D. Researcher. His current research interests are focused on the Internet of Health Things (IoHT) and biomedical signal processing, particularly in analyzing heart rate variability for specific applications such as stress, critical care, and sleep apnea. Additionally, he is working on the implementation of algorithms to detect drowsiness while driving.

EDUARDO GIL received the M.Sc. degree in telecommunication engineering from the University of Zaragoza (UZ), in 2002, the master's degree in sleep: physiology and medicine from the Pablo de Olavide University of Seville, in 2007, and the Ph.D. degree in biomedical engineering from UZ, in 2009. He is currently a Full Professor with the Department of Computer Science and Systems Engineering, conducting research at the Aragon Institute of Engineering Research (I3A) and the Biomedical Research Networking Center in Bioengineering, Biomaterials and Nanomedicine (CIBER-BBN). His research interests include biomedical signal processing, with specific interests in cardiovascular and respiratory dynamics and photoplethysmographic signal analysis.

JESÚS LÁZARO received the M.Sc. degree in telecommunication engineering, the M.Sc. degree in biomedical engineering, and the Ph.D. degree (cum laude) in biomedical engineering (International Doctor) from the University of Zaragoza, in 2011, 2012, and 2015, respectively. His postdoctoral work included positions at KU Leuven and the University of Connecticut, where he led the EU-funded WECARMON Project on wearable monitoring of cardiorespiratory diseases. Since 2024, he has been an Associate Professor at the Department of Computer Science and Systems Engineering, University of Zaragoza. His research interests include biomedical signal processing for personalized diagnosis and monitoring of cardiorespiratory patients.

RAQUEL BAILÓN (Member, IEEE) was born in Zaragoza, Spain, in 1978. She received the M.S. degree in telecommunication engineering and the Ph.D. degree in biomedical engineering from the University of Zaragoza (UZ), Zaragoza, Spain, in 2001 and 2006, respectively. In 2003, she was an Assistant Professor at the Department of Electronic Engineering and Communications, UZ, where she is currently a Full Professor. She is also a Researcher with the Aragon Institute for Engineering Research, UZ, and also with the Centro de Investigación Biomédica en Red en Bioingeniería, Biomateriales y Nanomedicina, Spain. Her current research interests include the biomedical signal processing field, especially in the analysis of the dynamics and interactions of cardiovascular signals.